Proceedings of the Eighteenth International Conference on
Civil, Structural and Environmental Engineering Computing
Edited by: P. Iványi, J. Kruis and B.H.V. Topping
Civil-Comp Conferences, Volume 10, Paper 15.2
Civil-Comp Press, Edinburgh, United Kingdom, 2025
ISSN: 2753-3239, doi: 10.4203/ccc.10.15.2

Flow and Species Transport in Soft Deforming Porous Medium; Homogenization Based Numerical Modelling

E. Rohan and F. Moravcová

Department of Mechanics, University of West Bohemia, Pilsen, Czech Republic

Abstract

The paper is aimed to explore influence of the fluid-structure interaction (FSI) in soft porous structure on the flow and tansport of a species agent to the solid while taking into account the interface permeability depending on the wall shear stress due to the flow. The modelling is based on the two-scale homogenization of the coupled FSI and the advection-diffusion problems. The solid skeleton is composed of rigid frame supporting a very compliant elastic, or poroelastic structure. The solid elasticity progressively less stiff with decreasing microstructure scale. This leads to the FSI tight coupling at the micro-scale, in contrast with the "standard"case of a given fixed elasticity. For the scale decoupling of the limit advection term in the two-scale trasport equation, the spectral based decomposition is proposed to avoid the use of the Laplace transformation of the product of two time functions. Finite element method is applied to solve both the micro- and macrosscopic problems of the flow and transport. Convolution kernels approximations are based on the Prony series to provide efficient integration schemes. Numerical illustrations are reported.

Keywords: multiscale modelling, porous media, advection-diffusion, asymptotic homogenization, semipermeable interface, fluid-structure interaction, dynamic permeability

1 Introduction

Transport in fluid saturated porous media is one of the most important classic problems of continuum mechanics. Although it has been thoroughly studied especially in the framework of the phenomenological approaches, there are still many modelling issues which require more accurate treatment to respect influence of given specific microstructure features on the effective behaviour observed at the macroscopic level. Based on the microstructure periodicity the homogenization method and its numerical implementation present one of the best modelling approaches in the sense of the a balance between the detail treatment of the coupled interactions between the fluid and solid phases, on one hand, and the computational robustness and efficiency, on the other hand.

The modelling approach employed in this study is based on the authors' recent works, namely those related to nonstationary fluid structure interaction and homogenization [1, 2] and [3]. We focus on linearized problem, however nonlinear formulations were considered *e.g.* in [2] and [4]. Further issues related to this paper include homogenization of species transport in heterogeneous structures with advection effects due to the Darcy and Stokes flows [5], influence of evolving microstructures [6], and large contrast in material parameters at the microstructure level. This latter issue was treated in [7] introducing thus the double porosity scaling ansatz, [8] focusing on the pressure discontinuity at interfaces, cf. [9].

In this short paper, we introduce the problem of interest defined the porous medium. The studied processes at the heterogeneity level (in the microstructure) involve the viscous fluid flow in a compliant skeleton stiffened by a rigid frame. Besides modelling the fluid-structure interactions, we are interested in the transport of a solvent due to the advection-diffusion processes in the fluid part and diffusion in the solid phase. The derived two-scale model of these coupled processes is briefly reported in terms the macroscopic model equations and the involved homogenized model parameters describing effective properties of the porous medium.

2 Two-scale model of transport in porous structure

We consider microstructures constituted by soft elastic skeleton supported by an embedded rigid scaffolds. In 3D, all the 3 phases, *i.e.* the fluid *(index f)*, a very soft - compliant elastic solid *(index c)* and the rigid structure - "the matrix" *(index m)* can be connected (each one).

The flow and species transport is described in domain $\Omega \subset \mathbb{R}^3$ decomposed into three principal parts

$$\Omega = \Omega_f^\varepsilon \cup \Omega_c^\varepsilon \cup \Omega_m^\varepsilon \cup \Gamma_{\rm fc}^\varepsilon \cup \Gamma_{\rm mc} \;, \quad \Omega_f^\varepsilon \cap \Omega_c^\varepsilon = \emptyset \;; \quad \Omega_c^\varepsilon \cap \Omega_m^\varepsilon = \emptyset \;, \tag{2.1}$$

where $\Gamma_{\rm fc}^\varepsilon$ and $\Gamma_{\rm mc}$ are the interfaces between the fluid and the elastic solid, and between the elastic solid and the rigid frame.

The microstructure heterogeneity is assumed to be periodic (or locally periodic) given by the representative volume element (RVE) defined using periodic unit cell Y, subject to the following decomposition, see Fig. 1

$$
\begin{aligned}
Y &= Y_f \cup Y_s \cup \Gamma_{\rm fs}\;, \;\text{ where } \Gamma_{\rm fs} = \partial Y_f \cap \partial Y_s\;,\\
Y_s &= Y_c \cup Y_m \cup \Gamma_{cm}\;, \;\text{ where } \Gamma_{cm} = \partial Y_c \cap \partial Y_m\;.
\end{aligned}
\tag{2.2}
$$

We assume Y_c separating the fluid and the "matrix", so that $\partial Y_f \cap \partial Y_m = \emptyset$, although this assumption is not crucial. We shall use also $Y_{fc} = Y_f \cup Y_c$ in the context of volume integrals. By virtue of the homogenization modelling technique based on the asymptotic analysis [10], the mathematical model represented by a system of PDEs parameterized by the scale $\varepsilon = \ell/L$ relating the micro- and macroscopic characteristic lengths. In the limit $\varepsilon \to 0$, we obtain a two-scale problem which can be decomposed into so-called local problems solved in the Y, and the macroscopic problem introduced in terms of the PDEs involving homogenized material coefficients.

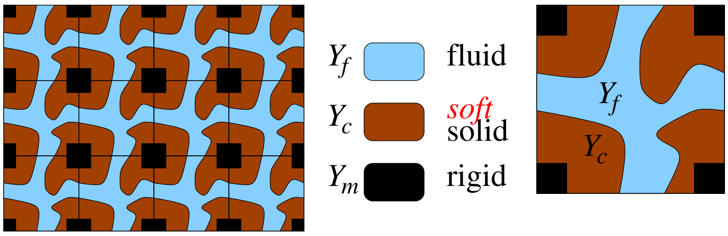

Figure 1: The periodic structure consisting of the fluid and a soft solid skeleton anchored in a rigid frame.

Material properties of the heterogeneous structure We consider a soft elastic phase characterized by stiffness tensor $\mathbb{D}^{c,\varepsilon} = \varepsilon^2 \bar{\mathbb{D}}^c$ and the density ρ^c. The Newtonian fluid in pores is slightly compressible, characterized by the bulk stiffness k_f, and by the viscosity tensor $\mathbb{D}^{f,\varepsilon} = \varepsilon^2 \bar{\mathbb{D}}^f$ given by $D^{f,\varepsilon}_{klij} = \mu^\varepsilon(\delta_{ik}\delta_{jl} + \delta_{il}\delta_{jk} - (2/3)\delta_{ij}\delta_{kl})$, where μ^ε is the dynamic viscosity, $\mu^\varepsilon = \varepsilon^2 \bar{\mu}$.

The periodic structure is characterized large contrast in the diffusivity coefficients. In particular, the diffusivity in the solid skeleton is much smaller than the one in the fluid. Accordingly, also the advection velocity in the dual porosity of skeleton Ω_s^ε is scaled by ε. The advection is relevant to the fluid in Ω_f^ε, whereas there is no flow in the solid Ω_s^ε.

$$
\begin{aligned}
\mathcal{T}_\varepsilon(\boldsymbol{w}^\varepsilon(x)) &= \left\{ \begin{array}{ll} \bar{\boldsymbol{w}}(x,y) & y \in Y_f\;,\\ 0 & y \in Y_s\;, \end{array}\right.\\
\mathcal{T}_\varepsilon(\boldsymbol{D}^\varepsilon(x)) &= \left\{ \begin{array}{ll} \bar{\boldsymbol{D}}(x,y) & y \in Y_f\;,\\ \varepsilon^2 \hat{\boldsymbol{D}}(x,y) & y \in Y_s\;, \end{array}\right.\\
\mathcal{T}_\varepsilon(\kappa_\theta^\varepsilon(x)) &= \varepsilon \bar{\kappa}_\theta(x,y), \quad y \in \Gamma_Y\;.
\end{aligned}
\tag{2.3}
$$

The scaling of the interface diffusivity $\kappa_\theta^\varepsilon(x)$ by ε is the consequence of the surface and volume measures; obviously $|\Omega_f^\varepsilon|/|\Gamma^\varepsilon| \sim 1/\varepsilon$.

2.1 Micromodel and interactions at pore level

We study fluid-structure interaction described by the displacement $\boldsymbol{u}^\varepsilon$ of the solid phase and by the fluid velocity $\boldsymbol{v}^{f,\varepsilon}$ in the channel. The transport of a species represented by its concentration θ^ε. It is useful to introduce the kinematic decomposition of the flow: fluid velocity $\boldsymbol{v}^{f,\varepsilon} = \boldsymbol{w}^\varepsilon + \tilde{\dot{\boldsymbol{u}}}^\varepsilon$, where $\boldsymbol{w}^\varepsilon = \mathbf{0}$ on Γ_{fc}^ε. By $\tilde{}$ we denote a (smooth) extension of vectorial field (displacement) from Y_c to Y_f. However, for the sake of brevity, we may often drop the "tilde" when referring to $\boldsymbol{u}$ extended into Y_f. The homogenization is applied to the following weak problem formulations of the flow, deformation and transport.

- The solid deformations: the displacement field $\boldsymbol{u}^\varepsilon \in U(\Omega_c^\varepsilon) = \{\boldsymbol{v} \in \mathbf{H}^1(\Omega_c^\varepsilon) | \boldsymbol{v} = 0 \text{ on } \Gamma_{cm}^\varepsilon\}$

$$\int_{\Omega_c^\varepsilon} \varepsilon^2 \bar{\mathbb{D}}^c \boldsymbol{e}(\boldsymbol{u}^\varepsilon) : \boldsymbol{e}(\boldsymbol{v}) + \int_{\Omega_c^\varepsilon} \rho_c^\varepsilon \ddot{\boldsymbol{u}}^\varepsilon \cdot \boldsymbol{v} - \int_{\Gamma_{fc}^\varepsilon} \boldsymbol{v} \cdot \boldsymbol{\sigma}^{f,\varepsilon} \cdot \boldsymbol{n}^c \mathrm{dS} = \int_{\Omega_c^\varepsilon} \boldsymbol{v} \cdot \boldsymbol{f}^{c,\varepsilon} \;, \quad (2.4)$$

  for all $\boldsymbol{v} \in U(\Omega_c^\varepsilon)$.

- The fluid flow: seepage velocity $\boldsymbol{w}^\varepsilon \in W(\Omega_f^\varepsilon) = \{\boldsymbol{v} \in \mathbf{H}^1(\Omega_f^\varepsilon) | \boldsymbol{v} = 0 \text{ on } \Gamma_{\rm fs}^\varepsilon\}$ and the fluid pressure $p^\varepsilon \in L^2(\Omega_f^\varepsilon)$ satisfy

$$\int_{\Omega_f^\varepsilon} \varepsilon^2 \bar{\mathbb{D}}^f \boldsymbol{e}(\boldsymbol{w}^\varepsilon + \dot{\boldsymbol{u}}^\varepsilon) : \boldsymbol{e}(\boldsymbol{\vartheta}) - \int_{\Omega_f^\varepsilon} p^\varepsilon \nabla \cdot \boldsymbol{\vartheta} + \int_{\Omega_f^\varepsilon} \rho_0 (\dot{\boldsymbol{w}}^\varepsilon + \ddot{\boldsymbol{u}}^\varepsilon) \cdot \boldsymbol{\vartheta} = \int_{\Omega_f^\varepsilon} \boldsymbol{\vartheta} \cdot \boldsymbol{f}^{f,\varepsilon} \;,$$
$$\int_{\Omega_f^\varepsilon} q \left(\dot{p}^\varepsilon + k_f \nabla \cdot (\boldsymbol{w}^\varepsilon + \dot{\boldsymbol{u}}^\varepsilon) \right) = 0 \;, \quad (2.5)$$

  for all $\boldsymbol{\vartheta} \in W(\Omega_f^\varepsilon)$ and all $q \in L^2(\Omega_f^\varepsilon)$. The solid displacement $\boldsymbol{u}^\varepsilon$ is assumed to be extended smoothly in Ω_f^ε.

- The species transport : Find $\theta^\varepsilon \in \hat{V}_*^\varepsilon(\Omega)$, such that

$$\begin{aligned} &\int_\Omega \partial_t \theta^\varepsilon \psi^\varepsilon + \int_\Omega (\boldsymbol{D}^\varepsilon \nabla \theta^\varepsilon - \theta^\varepsilon \boldsymbol{w}^\varepsilon) \cdot \nabla \psi^\varepsilon + \int_{\Gamma_{\rm fc}^\varepsilon} \kappa_\theta^\varepsilon [\theta^\varepsilon]_{\Gamma^\varepsilon} [\psi^\varepsilon]_{\Gamma^\varepsilon} \\ &= \int_\Omega f^\varepsilon \psi^\varepsilon + \int_{\partial\Omega} (\boldsymbol{D}^\varepsilon \nabla \theta^\varepsilon - \theta^\varepsilon \boldsymbol{w}^\varepsilon) \cdot \boldsymbol{n} \psi^\varepsilon \, \mathrm{d}S \;, \quad \forall \psi^\varepsilon \in \hat{V}_0^\varepsilon(\Omega) \end{aligned} \quad (2.6)$$

2.2 Homogenization using asymptotic expansions

The homogenization applied the limit two-scale model is based on the periodic unfolding method. The resulting equations can obtained formally using truncated asymptotic expansions considered for all the involved fields; due to the decomposition (2.1) and

(2.2) we get (note $\boldsymbol{u}^1$ is extended to the fluid domain)

$$
\begin{aligned}
\mathcal{T}_\varepsilon(\boldsymbol{u}^\varepsilon(x,t)) &= \hat{\boldsymbol{u}}^0(x,y,t) + \varepsilon \boldsymbol{u}^1(x,y,t)\;, \quad y \in Y_c \cup Y_f\;,\\
\mathcal{T}_\varepsilon(\boldsymbol{w}^\varepsilon(x,t)) &= \hat{\boldsymbol{w}}^0(x,y,t) + \varepsilon \boldsymbol{w}^1(x,y,t)\;, \quad y \in Y_f\;,\\
\mathcal{T}_\varepsilon(p_d^\varepsilon(x,t)) &= p_d^0(x,t) + \varepsilon p_d^1(x,y,t)\;, \quad y \in Y_d, \quad d = c, f\;,\\
\mathcal{T}_\varepsilon(\theta^\varepsilon(x,t)) &= \chi_f(y)[\theta_f^0(x,t) + \varepsilon\theta_f^1(x,y,t)] + \chi_s\hat{\theta}(x,y,t)\;,
\end{aligned}
\tag{2.7}
$$

where χ_d is the characteristic function of domain Y_d, $d = f, s$; the fluctuations $\boldsymbol{u}^1$ and $\boldsymbol{w}^1$ are irrelevant for the 1st order homogenization. Upon substituting (2.7) in the unfolded equations obtained from formulations (2.4), (2.5), and (2.6), the limit equations are obtained by letting $\varepsilon \to 0$. For this, analogous ansatz for the test functions involved in the weak formulations is used, as the one in (2.7). Then, due to the system linearity, a multiplicative decomposition of the two-scale solutions $\hat{\boldsymbol{u}}^0, \hat{\boldsymbol{w}}^0, p_d^1$ and $\theta_f^1, \hat{\theta}$ into the macroscopic functions and autonomous characteristic responses is introduced in terms of the Laplace transformation in time, which yields the two-scale functions

$$
\begin{aligned}
\hat{\boldsymbol{w}}^0(t,x,y) &= \int_0^t \boldsymbol{w}^k(t-\tau,y)\partial_\tau\partial_k^x p^0(t,x)\mathrm{d}\tau\;, \quad y \in Y_f\;,\\
\hat{\boldsymbol{u}}^0(t,x,y) &= \int_0^t \boldsymbol{\chi}^k(t-\tau,y)\partial_\tau\partial_k^x p^0(t,x)\mathrm{d}\tau\;, \quad y \in Y_c\\
p_d^1(x,y,t) &= \int_0^t \pi^k(t-\tau,y)\partial_\tau\partial_k^x p^0(t,x)\mathrm{d}\tau\;, \quad y \in Y_d\;,\ d = c, f\;,
\end{aligned}
\tag{2.8}
$$

and, in analogy, also for θ_f^1 and $\hat{\theta}$; details are skipped here, see below.

2.3 Flow problem – two-scale limit model

The resulting model consists of the characteristic autonomous problems and the macroscopic equation attaining the form of a non-stationary Darcy flow.

Characteristic responses for the fluid flow The weak formulation of the local problem involves bilinear forms associated with the soft elasticity in Y_c, viscous fluid dissipation in Y_f, inertia of both the solid and fluid, and the inner products, defined as follows

$$
\begin{aligned}
a_c\left(\boldsymbol{u},\,\boldsymbol{v}\right) &= \int_{Y_c} \bar{\mathbb{D}}^c \boldsymbol{e}_y(\boldsymbol{u}) : \boldsymbol{e}_y(\boldsymbol{v})\;,\\
a_f\left(\boldsymbol{w},\,\boldsymbol{v}\right) &= \bar{\mu}\int_{Y_f} \nabla_y \boldsymbol{w} : \nabla_y \boldsymbol{v}\;,\\
\varrho_f\left(\boldsymbol{u},\,\boldsymbol{v}\right) &= \int_{Y_c} \rho_c \boldsymbol{u}\cdot\boldsymbol{v}\;,\\
\langle p,\,q\rangle_{Y_f} &= \int_{Y_f} pq\;,\\
\langle \boldsymbol{u},\,\boldsymbol{v}\rangle_{Y_c} &= \int_{Y_c} \boldsymbol{u}\cdot\boldsymbol{v}\;,\ \text{where}\ \int_{Y_d} = \frac{1}{|Y|}\int_{Y_d}\;.
\end{aligned}
\tag{2.9}
$$

The following spaces are employed: $\mathbf{H}^1_{\#}(Y)$ is the Sobolev space of vector-valued Y-periodic functions (the subscript $\#$). Further $\mathbf{H}^1_{\#0}(Y_f)$ is restricted to the fields wit vanishing trace on $\Gamma_{\rm fc}$, the channel wall. We employ spaces of admissible displacements, $\boldsymbol{U}(Y_{fc}) = \mathbf{H}^1_{\#}(Y_c)\cap\mathbf{H}^1_{\#0}(Y_{fc})$ and $\tilde{\boldsymbol{U}}(Y_{fc}) = \{\boldsymbol{v}\in\boldsymbol{U}(Y_{fc})|\ \nabla_y\cdot\boldsymbol{v} = 0\ \text{ in } Y_f\}$, and the space of admissible pressure, $Q(Y_{fc}) = L^2(Y_{fc})\cap(H^1_{\#}(Y_f)\cup H^1_{\#}(Y_c))$.

The characteristic autonomous responses of the microstructure with respect to unit macroscopic pressure gradients must be computed by solving the following problem.

Find $(\boldsymbol{\chi}^k(t,y),\boldsymbol{w}^k(t,y),\pi^k(t,y))\in\tilde{\boldsymbol{U}}(Y_{fc})\times\mathbf{H}^1_{\#0}(Y_f)\times Q(Y_{fc})$ for $t>0$, satisfying zero initial conditions, $(\boldsymbol{\chi}^k(0,y),\boldsymbol{w}^k(0,y),\pi^k(0,y)) = 0$, and $\partial_t\boldsymbol{\chi}^k(0,y) = 0$, such that

$$
\begin{aligned}
& a_c\left(\boldsymbol{\chi}^k,\,\boldsymbol{v}\right) + a_f\left(\boldsymbol{w}^k + \partial_t\boldsymbol{\chi}^k,\,\tilde{\boldsymbol{v}}\right) - \left\langle\pi^k,\,\nabla_y\cdot\tilde{\boldsymbol{v}}\right\rangle_{Y_c\cup Y_f}\\
&\quad + \rho_0\left\langle\partial_t\boldsymbol{w}^k + \partial_{tt}\boldsymbol{\chi}^k,\,\tilde{\boldsymbol{v}}\right\rangle_{Y_f} + \varrho_c\left(\partial_{tt}\boldsymbol{\chi}^k,\,\boldsymbol{v}\right) = -H_+(t)\left\langle\mathbf{1}^k,\,\tilde{\boldsymbol{v}}\right\rangle_{Y_c\cup Y_f}\;,\\
& a_f\left(\boldsymbol{w}^k + \partial_t\boldsymbol{\chi}^k,\,\boldsymbol{\vartheta}\right) - \left\langle\pi^k,\,\nabla_y\cdot\boldsymbol{\vartheta}\right\rangle_{Y_f} + \rho_0\left\langle\partial_t\boldsymbol{w}^k + \partial_{tt}\boldsymbol{\chi}^k,\,\boldsymbol{\vartheta}\right\rangle_{Y_f} = -H_+(t)\left\langle\mathbf{1}^k,\,\boldsymbol{\vartheta}\right\rangle_{Y_f}\;,\\
& \left\langle q,\,\nabla_y\cdot(\boldsymbol{w}^k + \partial_t\boldsymbol{\chi}^k)\right\rangle_{Y_f} = 0\;,\\
& \left\langle q,\,\nabla_y\cdot\boldsymbol{\chi}^k\right\rangle_{Y_c} = 0\;,
\end{aligned}
\tag{2.10}
$$

for all $\tilde{\boldsymbol{v}}\in\tilde{\boldsymbol{U}}(Y_{fc})$, $\boldsymbol{\vartheta}\in\mathbf{H}^1_{\#0}(Y_f)$, and $q\in Q(Y_{fc})$. Above, $H_+(t)$ is the Heaviside function.

Macroscopic flow model The macroscopic problem in time domain attains the following form: given an initial state $p(0,x) = \bar{p}(x)$, $x\in\Omega$, find pressure $p^0\in H^1(\Omega)$, such that $p^0 = p^\partial$ on $\partial_p\Omega\subset\partial\Omega$ satisfies

$$
\mathcal{C}\partial_t p^0 + \nabla_x\cdot\int_0^t \widehat{\boldsymbol{\mathcal{K}}}(t-\tau)\frac{\partial}{\partial\tau}\left(\bar{\boldsymbol{f}}(\tau,\cdot) - \nabla_x p^0(\tau,\cdot)\right)\mathrm{d}\tau\;,\quad \text{a.e. in}\ \Omega\;,
\tag{2.11}
$$

involving the homogenized coefficients $\widehat{\boldsymbol{\mathcal{K}}}$ and $\mathcal{C}$.

The dynamic permeability $\widehat{\boldsymbol{\mathcal{K}}}(t) = \widehat{\mathcal{K}}_{ij}(t)$ constitutes a convolution kernel in (2.11). It is introduced using the average of the total fluid velocity in the fluid channels,

$$\begin{aligned} \widehat{\mathcal{K}}_{kj}(t) &= -\left\langle \mathbf{1}^k,\, \boldsymbol{w}^j \right\rangle_{Y_f} - \left\langle \mathbf{1}^k,\, \partial_t \tilde{\boldsymbol{\chi}}^j \right\rangle_{Y_c \cup Y_f} \\ &= a_c\left(\boldsymbol{\chi}^k,\, \partial_t \boldsymbol{\chi}^j\right) + a_f\left(\boldsymbol{w}^k + \partial_t \tilde{\boldsymbol{\chi}}^k,\, \boldsymbol{w}^j + \partial_t \tilde{\boldsymbol{\chi}}^j\right) \\ &\quad + \rho_0 \left\langle \partial_t \boldsymbol{w}^k + \partial_{tt} \tilde{\boldsymbol{\chi}}^k,\, \boldsymbol{w}^j + \partial_t \tilde{\boldsymbol{\chi}}^j \right\rangle_{Y_f} + \varrho_c\left(\partial_{tt} \boldsymbol{\chi}^k,\, \partial_t \boldsymbol{\chi}^j\right) \,. \end{aligned} \tag{2.12}$$

Moreover, a symmetric expression can be obtained in the Laplace-time domain,

$$\begin{aligned} \underset{*}{\widehat{\mathcal{K}}}_{kj}(\lambda) &= -\left\langle \mathbf{1}^k,\, \underset{*}{\boldsymbol{w}}^j \right\rangle_{Y_f} - \lambda \left\langle \mathbf{1}^k,\, \underset{*}{\tilde{\boldsymbol{\chi}}}^j \right\rangle_{Y_c \cup Y_f} \\ &= \lambda^2 a_c\left(\underset{*}{\boldsymbol{\chi}}^k,\, \underset{*}{\boldsymbol{\chi}}^j\right) + \lambda a_f\left(\underset{*}{\boldsymbol{w}}^k + \lambda \underset{*}{\tilde{\boldsymbol{\chi}}}^k,\, \underset{*}{\boldsymbol{w}}^j + \lambda \underset{*}{\tilde{\boldsymbol{\chi}}}^j\right) \\ &\quad + \lambda^2 \rho_0 \left\langle \underset{*}{\boldsymbol{w}}^k + \lambda \underset{*}{\tilde{\boldsymbol{\chi}}}^k,\, \underset{*}{\boldsymbol{w}}^j + \lambda \underset{*}{\tilde{\boldsymbol{\chi}}}^j \right\rangle_{Y_f} + \lambda^4 \varrho_c\left(\underset{*}{\boldsymbol{\chi}}^k,\, \underset{*}{\boldsymbol{\chi}}^j\right) \,. \end{aligned} \tag{2.13}$$

The bulk material is compressible, characterized by the effective compressibility

$$\mathcal{C} = \frac{\phi_f}{k_f} + \int_{Y_c} \frac{1}{k_c} \,. \tag{2.14}$$

2.4 Species concentration – trasport problem

The two-scale concentrations defined in the fluid and solid parts are expressed in terms of characteristic responses which are needed to compute the homogenized coefficients of the macroscopic transport equation.

Characteristic responses for the species transport in the fluid channels Y_f The local concentration in the channel is governed by the following limit transport equation

$$-\int_{Y_f} \theta_f^0 \hat{\boldsymbol{w}} \cdot \nabla_y \psi + \int_{Y_f} \bar{\boldsymbol{D}}(\nabla_y \theta_f^1 + \nabla_x \theta_f^0) \cdot \nabla_y \psi = 0 \,, \quad \forall \psi \in H^1_\#(Y_f) \,, \tag{2.15}$$

where the advection velocity is the two-scale function $\hat{\boldsymbol{w}}(t, x, y)$ given for in $y \in Y_f$ by the solution p^0 of (2.11). Recall $\hat{\boldsymbol{w}}$ is expressed in terms of the time convolution, involving $\boldsymbol{w}^k$, the solution of (2.10). To introduce the characteristic concentration responses of the microstructure independently of the macroscopic fields, namely θ_f^0 and $\partial_k^x p^0$, we use the approach based on the spectral decomposition of the diffusion operator.

Consider the following eigenvalue problem: find $(\eta^r, \vartheta^r) \in \mathbb{R} \times H^1_\#(Y_f)$, such that, for $r = 1, 2, \ldots$,

$$\begin{aligned} \int_{Y_f} (\bar{\boldsymbol{D}} \nabla_y \vartheta^r) \cdot \nabla_y \psi = \eta^r \left\langle \vartheta^r,\, \psi \right\rangle_{Y_f} \,, \quad \forall \psi \in H^1_\#(Y_f) \,, \\ \left\langle \vartheta^r,\, \vartheta^s \right\rangle_{Y_f} = \delta_{rs} \,. \end{aligned} \tag{2.16}$$

Using the projection in the basis $\{\vartheta^r\}$ defined due to (2.16), we can introduce coefficients $b^r_w(t,x)$ and $b^r_\nabla(t,x)$, such that

$$\begin{aligned}\theta_f^{1,w}(t,x,y) &= \sum_r b^r_w(t,x)\vartheta^r(y)\;,\\ \theta_f^{1,\nabla}(t,x,y) &= \sum_r b^r_\nabla(t,x)\vartheta^r(y)\;,\end{aligned} \tag{2.17}$$

where b^r_∇ is given by the diffusion flux,

$$\begin{aligned}b^r_\nabla(t,x) &= \sum_k \bar{b}^r_{k,\nabla}\partial^x_k\theta^0_f(t,x)\;,\\ \bar{b}^r_{k,\nabla} &= -\frac{1}{\eta^r}\int_{Y_f}(\bar{\boldsymbol{D}}\nabla_y\vartheta^r)_k\;,\end{aligned} \tag{2.18}$$

wherease $b^r_w(t,x)$ is due to the advection velocity,

$$\begin{aligned}b^r_w(t,x) &= \sum_k \tilde{b}^r_{k,w}(t,x)\theta^0_f(t,x)\;,\\ c^r_k(t) &= \frac{1}{\eta^r}\int_{Y_f}\boldsymbol{w}^k(t,y)\cdot\nabla_y\vartheta^r(y)\mathrm{d}y\;,\\ \tilde{b}^r_{k,w}(t,x) &= \int_0^t c^r_k(t-\tau)\partial_\tau\partial^x_k p^0(\tau,x)\mathrm{d}\tau\;.\end{aligned} \tag{2.19}$$

Characteristic responses for the species diffusion in the solid Y_s In the skeleton, assuming no advection, the local problem describes a non-stationary diffusion. We consider the case of interfaces Γ_{fc} with a reduced diffusivity which yields the interface intergral in (2.6), hence, the discontinuity of the concentration, $\hat{\theta}(t,x,\cdot)\neq\theta^0_f(t,x)$ and the associated test functions. The local problem is nonstationary, in general,

$$\left\langle\partial_t\hat{\theta},\,\hat{\psi}\right\rangle_{Y_s}+\int_{Y_s}(\hat{\boldsymbol{D}}\nabla_y\hat{\theta})\cdot\nabla_y\hat{\psi}+\int_{\Gamma_{\mathrm{fs}}}\bar{\kappa}_\theta\hat{\theta}\hat{\psi}=\int_{\Gamma_{\mathrm{fs}}}\bar{\kappa}_\theta\theta^0_f\hat{\psi}\;,\quad\forall\hat{\psi}\in H^1_\#(Y_s)\;. \tag{2.20}$$

Upopn introducing the characteristic responses $\bar{\vartheta}^0_f(y)$ and $\tilde{\vartheta}_f(t,y)$, the species concentration in the solid, $\hat{\theta}$, is expressed by the time convolution

$$\begin{aligned}\hat{\theta}(t,x,\cdot) &= \tilde{\theta}(t,x,\cdot)+\hat{\theta}^0(x,\cdot)\\ &= \int_0^t\tilde{\vartheta}^0_f(t-\tau,\cdot)\partial_\tau\theta^0_f(\tau,x)\mathrm{d}\tau+\bar{\vartheta}^0_f\,\bar{\theta}^0_f(x)\;.\end{aligned} \tag{2.21}$$

The characteristic responses $\bar{\vartheta}^0_f$ and $\tilde{\vartheta}^0_f$ are solutions of the following two local problems:

1. Find $\bar{\vartheta}_f^0 \in H^1_\#(Y_s)$ satisfying

$$\int_{Y_s} (\hat{\boldsymbol{D}} \nabla_y \bar{\vartheta}_f^0) \cdot \nabla_y \hat{\psi} + \int_{\Gamma_{\rm fs}} \bar{\kappa}_\theta \bar{\vartheta}_f^0 \hat{\psi} = \int_{\Gamma_\beta} \bar{\kappa}_\theta \hat{\psi} {\rm dS}_y \;, \quad \forall \hat{\psi} \in H^1_\#(Y_s) \;. \quad (2.22)$$

2. Find $\tilde{\vartheta}_f^0(t,\cdot) \in H^1_\#(Y_s)$, such that $\tilde{\vartheta}_f^0(0,\cdot) = 0$ in Y_s, satisfying

$$\left\langle \partial_t \tilde{\vartheta}_f^0, \, \hat{\psi} \right\rangle_{Y_s} + \int_{Y_s} (\hat{\boldsymbol{D}} \nabla_y \tilde{\vartheta}_f^0) \cdot \nabla_y \hat{\psi} + \int_{\Gamma_{\rm fs}} \bar{\kappa}_\theta \tilde{\vartheta}_f^0 \hat{\psi} = \int_{\Gamma_\beta} \bar{\kappa}_\theta \hat{\psi} {\rm dS}_y \;, \quad \forall \hat{\psi} \in H^1_\#(Y_s) \;. \quad (2.23)$$

Macroscopic model of the transport problem The macroscopic concentration θ_f^0 is governed by transport equation which is obtained from (2.6) in the two-scale limit upon introducing there the homogenized coefficients defined below. The macroscopic problem becomes: Find $\theta_f^0(t,\cdot) \in V^f(\Omega)$ for any $t \geq 0$ which satisfy

$$\begin{aligned} & \int_\Omega \psi_f^0 \left[\phi_f \partial_t \tilde{\theta}_f^0 + \left(\bar{\mathcal{G}} \bar{\theta}_f^0 + \int_0^t \tilde{\mathcal{G}}(t-\tau) \frac{\rm d}{{\rm d}\tau} \tilde{\theta}_f^0(\tau) {\rm d}\tau \right) \right] \\ & + \int_{\partial\Omega} \boldsymbol{n} \cdot \bar{\boldsymbol{W}}^f \theta_f \psi_f {\rm d}S + \int_\Omega \nabla_x \psi_f^0 \cdot \left(\boldsymbol{\mathcal{D}} \nabla_x \theta_f^0 - \boldsymbol{\mathcal{W}} \theta_f^0 \right) = \int_\Omega \bar{f}_f \psi_f^0 \;, \end{aligned} \quad (2.24)$$

for all $\psi_f^0 \in V_0^f(\Omega)$.

The transport in the fluid channels is reflected by the effective diffusivity $\boldsymbol{\mathcal{D}} = (\mathcal{D}_{ij})$

$$\mathcal{D}_{ij} = \int_{Y_f} \bar{D}_{ij}^f - \sum_r \eta^r \bar{b}^r_{i,\nabla} \bar{b}^r_{j,\nabla} \;, \quad (2.25)$$

see (2.18), and the effective advection $\boldsymbol{\mathcal{W}} = (\mathcal{W}_i)$ which comprises the mean fluid velocity $\bar{\boldsymbol{W}}^f$ and also the non-stationary effect due to the flow,

$$\mathcal{W}_i = \int_{Y_f} \boldsymbol{w} - \int_{Y_f} (\bar{\boldsymbol{D}}^f \nabla_y \vartheta^r) \cdot \nabla_y y_i \int_0^t c_k^r(t-\tau) \partial_\tau \partial_k^x p^0(\tau, x) {\rm d}\tau \;. \quad (2.26)$$

The diffusion in the solid is represented by coefficients $\hat{\mathcal{G}}(t)$, such that

$$\begin{aligned} \hat{\mathcal{G}}(t) &:= \tilde{\mathcal{G}}(t) - \bar{\mathcal{G}} \;, \\ \text{where } \tilde{\mathcal{G}}(t) &= \int_{\Gamma_{\rm fs}} \bar{\kappa}_\theta \left(1 - \tilde{\vartheta}_f(t,y) \right) {\rm dS}_y \;, \\ \bar{\mathcal{G}} &= \int_{\Gamma_\alpha} \bar{\kappa}_\theta \left(1 - \bar{\vartheta}_f^0 \right) {\rm dS}_y \;, \end{aligned} \quad (2.27)$$

where the characteristic responses $\tilde{\vartheta}_f$ and $\bar{\vartheta}_f^0$ reflect the solid diffusivity $\hat{\boldsymbol{D}}$, including $\bar{\kappa}_\theta$, the one of the wall.

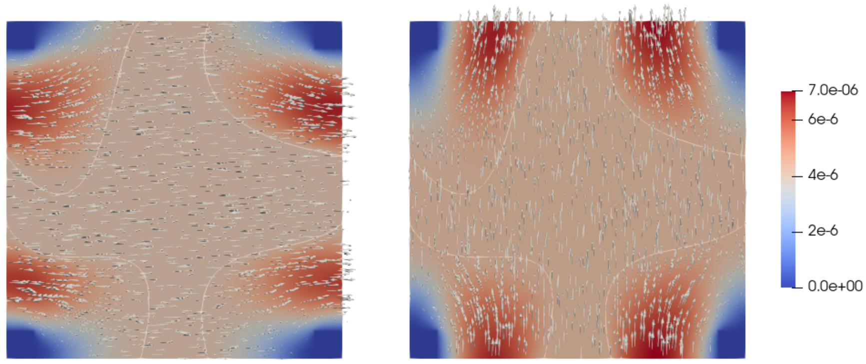

Figure 2: Steady characteristic displacements $\boldsymbol{\chi}^k$ in Y, coordinate modes $k = 1$ (left), $k = 2$ (right). Note that $\boldsymbol{\chi}^k$ in Y_f is defined as an extension from solid Y_c

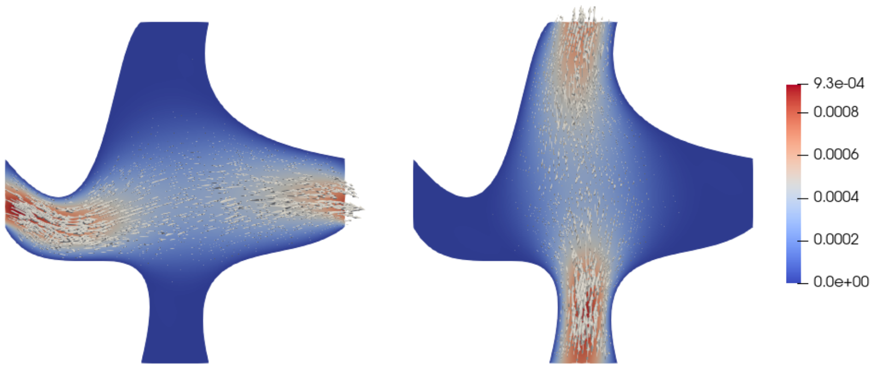

Figure 3: Steady characteristic velocities $\boldsymbol{w}^k$ in Y_f. coordinate modes $k = 1$ (left), $k = 2$ (right)

2.5 Numerical results – illustration

We consider a 2D microstructure whose the geometry is apparent from the pictures illustrating the characteristic responses, see Figs. 2-4. Although all the responses are time-dependent, the figures report distributions of $\boldsymbol{\chi}^k$, $\boldsymbol{w}^k$ and π^k for the steady state, $t \to \infty$. The mechanical properties of the solid and fluid phases are given in Tab. 1, where "shear stiffness in Y_f" is employed to define the smooth extension of displacements from solid Y_c to fluid Y_f.

The transient response of the microstructure, namely the flow is characterized by the permeability serving the convolution kernel $\widehat{\mathcal{K}}_{ij}(t)$, see Fig. 5. For $t \to \infty$, $\widehat{\mathcal{K}}$, the static permeability $\bar{\mathcal{K}}$. The oscillations of the kernel are due to the inertia effects involved in the fluid-structure interaction in problem (2.10), decaying with time due to the viscous dissipation.

The macroscopic response is illustrated by a steady state flow in the homogenized medium characterized by the static permeability $\bar{\mathcal{K}}$. In Fig. 6, p^0 is displayed in rectangular domain $\Omega =]0, L_1[\times]0, L_2[$ with prescribed pressure on the left side, $p^0(x_1 = 0, x_2) = \cos(2\pi x_2/L_2)$ and right side $p^0(x_1 = L_1, x_2) = 0$, whereby

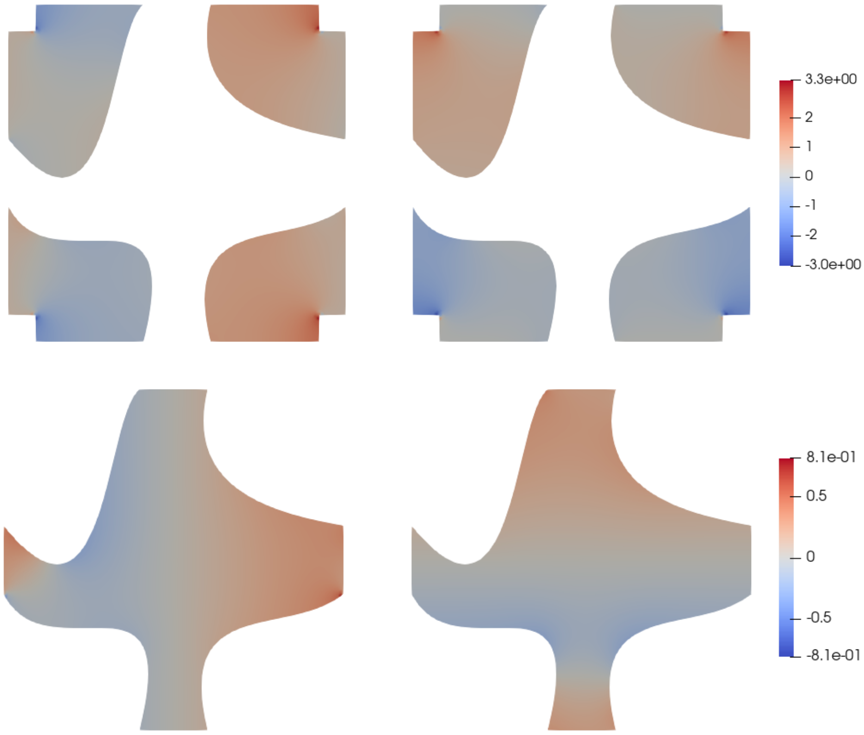

Figure 4: Steady characteristic pressures π^k in Y_c (top) and in Y_f (bottom) . Left: $k = 1$. Right: $k = 2$.

$\boldsymbol{n} \cdot \bar{\mathcal{K}} \nabla p^0 = 0$ is considered on the "upper" and "lower" sides, $x_2 = L_2$ and $x_2 = 0$. Fig. 7 shows the reconstruction of the fluid velocity in channels of the local microstructures at three different positions.

Fluid phase (water)	Elastic phase (bio tissue)	
$\bar{\mu} = 10$ Pa	$k_e = k_f$	Shear stiffness in Y_f
$\rho_f = 10^3$ kg/m^3	$\rho_e = \rho_f$	$G_f / G = 10^{-4}$
$k_f = 2.1\ 10^9$	$G = 10^8$ Pa	

Table 1: Simulation parameters and coefficients.

3 Concluding remarks

The objective of this short paper was to introduce the problem of the homogenization based multiscale modelling of viscous flows and advection-diffusion driven transport of species in porous structures featured by very soft elastic skeleton interacting with the fluid flow. By virtue of the asymptotic analysis concerning the scale $\varepsilon \to 0$ and the skeleton elasticity scaled by ε^2, the resulting limit microscopic problem to solve describes the tight fluid-structure interaction. This consequently influences the hy-

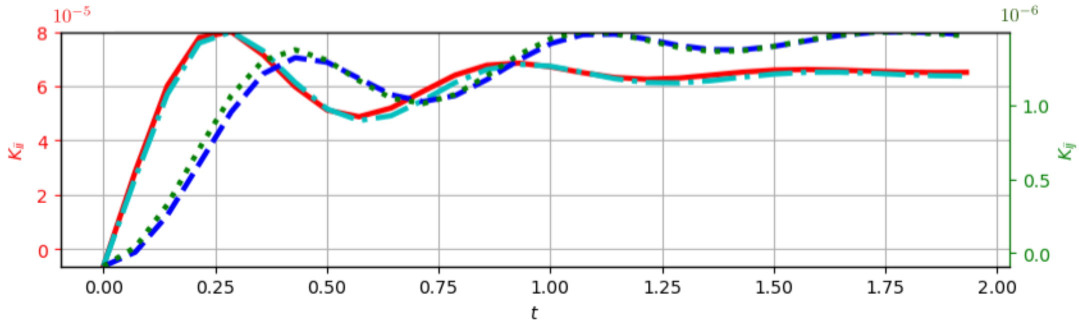

Figure 5: Time-evolution of the permeability component $\widehat{K}_{ij}$. The diagonal components are related to the right-hand axis scale ($\sim 10^{-5}$), the off-diagonal ones to the left-hand axis scale ($\sim 10^{-6}$).

draulic dynamic permeability which reflects mechanical properties of both the fluid and solid phases. The advection velocity field is involved in the transport problem. To treat nonstationary flow and species transport, we propose the spectral decomposition based decomposition of the concentration. This enables to avoid the use of the Laplace transformation of the product of two time functions. The derived homogenized transport reflects also the solid diffusivity including the fluid-solid interface. Although the presented problem is illustrated by applications in tissue engineering, the presented model can be developed further towards many other applications dealing with porous and compliant structures. As a further model extension towards such applications, the rigid frame Ω_m^ε of the skeleton will be replaced by an elastic one, but much stiffer than the soft material in Ω_c^ε.

Acknowledgements

The research has been supported by the grant project GA 24-12291S of the Czech Science Foundation.

References

[1] E. Rohan, S. Naili, Homogenization of the fluid-structure interaction in acoustics of porous media perfused by viscous fluid, ZAMP-Z Angew Math Phys 71 (4) (2020) 137–164.

[2] E. Rohan, V. Lukeš, Homogenized model of peristaltic deformation driven flows in piezoelectric porous media, Comput Struct 302 (2024) 107470.

[3] E. Rohan, F. Moravcová, Acoustic streaming in porous media – homogenization based two-scale modelling, Journal of Physics: Conference Series 2647 (23) (2024) 232009.

[4] D. Brown, P. Popov, Y. Efendiev, Effective equations for fluid-structure interaction with applications to poroelasticity, Appl Anal 93 (4) (2014) 771–790.

Figure 6: Macroscopic pressure p^0, in macroscopic domain $[L_1 \times L_2] = [1 \times 1.5]$, with the boundary condition $p^0(x_1 = 0, x_2) = \cos(2\pi x_2/L_2)$.

[5] Chavarría-Krauser, A., Ptashnyk, M., Homogenization approach to water transport in plant tissues with periodic microstructures, Math Model Nat Phenom 8 (4) (2013) 80–111.

[6] M. Gahn, M. Neuss-Radu, I. Pop, Homogenization of a reaction-diffusion-advection problem in an evolving micro domain and including nonlinear boundary conditions, Journal of Differential Equations 289 (2021) 95–127.

[7] T. Arbogast, J. Douglas, U. Hornung, Derivation of the double porosity model of single phase flow via homogenization theory, Siam J Math Anal 21 (4) (1990) 823–836.

[8] G. Griso, E. Rohan, Homogenization of diffusion-deformation in dual-porous medium with discontinuity interfaces, Asymptotic Anal 86 (2014) 59–98.

[9] Z. Li, D. Wang, X. Zhang, J. Crawford, Water flow across the interface of contrasting materials: Pressure discontinuity and its implications, J Hydrol 566 (2018) 435–440.

[10] D. Cioranescu, A. Damlamian, G. Griso, The Periodic Unfolding Method; Theory and Applications to Partial Differential Problems, Series in Contemporary Mathematics 3, Springer, 2018.

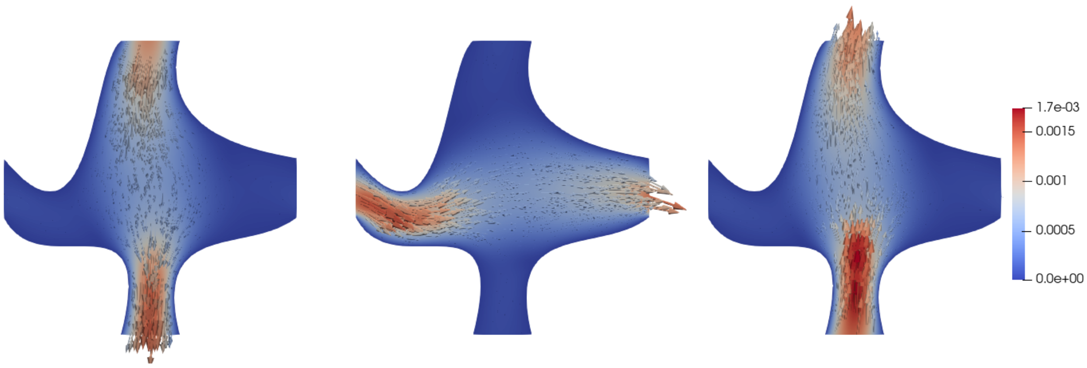

Figure 7: Advection velocity $\boldsymbol{w}$ at three macroscopic location on the same "vertical" line $x_2 = 0.2$. With the macro pressure distribution as shown in Fig.6. From left to right: $x = (0.2, 0.25)$ i.e. $\nabla p^0 = (-0.08, -1.64)$, $x = (0.2, 0.5)$ (x is on horizontal meridian) i.e. $\nabla p^0 = (1.65, 0.09)$, and $x = (0.2, 0.75)$ i.e. $\nabla p^0 = (-0.10, 1.92)$, with the macroscopic lengths size $L_1 = 1.5$ and $L_2 = 1$.